

## Identification of the Melatonin-binding Site $MT_3$ as the Quinone Reductase 2\*

Received for publication, June 14, 2000, and in revised form, July 19, 2000  
Published, JBC Papers in Press, July 25, 2000, DOI 10.1074/jbc.M005141200

Olivier Nosjean‡, Myriam Ferro§, Francis Cogé‡, Philippe Beauverger‡, Jean-Michel Henlin||, François Lefoulon||, Jean-Luc Fauchère||, Philippe Delagrance\*\*, Emmanuel Canet‡, and Jean A. Boutin‡ ‡‡

From the ‡Pharmacologie Moléculaire et Cellulaire, Institut de Recherches Servier, 78290 Croissy-sur-Seine, France, the §Laboratoire de Chimie des Protéines, CEA, 38000 Grenoble, France, the ¶Chimie Peptidique et Combinatoire, Institut de Recherches Servier, 92150 Suresnes, ||Technologie Servier, 45007 Orléans, France, and the \*\*Institut de Recherches Internationales Servier, 92415 Courbevoie, France

The regulation of the circadian rhythm is relayed from the central nervous system to the periphery by melatonin, a hormone synthesized at night in the pineal gland. Besides two melatonin G-coupled receptors,  $mt_1$  and  $MT_2$ , the existence of a novel putative melatonin receptor,  $MT_3$ , was hypothesized from the observation of a binding site in both central and peripheral hamster tissues with an original binding profile and a very rapid kinetics of ligand exchange compared with  $mt_1$  and  $MT_2$ . In this report, we present the purification of  $MT_3$  from Syrian hamster kidney and its identification as the hamster homologue of the human quinone reductase 2 (QR<sub>2</sub>, EC 1.6.99.2). Our purification strategy included the use of an affinity chromatography step which was crucial in purifying  $MT_3$  to homogeneity. The protein was sequenced by tandem mass spectrometry and shown to align with 95% identity with human QR<sub>2</sub>. After transfection of CHO-K1 cells with the human QR<sub>2</sub> gene, not only did the QR<sub>2</sub> enzymatic activity appear, but also the melatonin-binding sites with  $MT_3$  characteristics, both being below the limit of detection in the native cells. We further confronted inhibition data from  $MT_3$  binding and QR<sub>2</sub> enzymatic activity obtained from samples of Syrian hamster kidney or QR<sub>2</sub>-overexpressing Chinese hamster ovary cells, and observed an overall good correlation of the data. In summary, our results provide the identification of the melatonin-binding site  $MT_3$  as the quinone reductase QR<sub>2</sub> and open perspectives as to the function of this enzyme, known so far mainly for its detoxifying properties.

identified on pharmacological grounds, with lower melatonin affinity (nanomolar range), very rapid ligand association/dissociation kinetics, and an original pharmacological profile (4–6). In line with  $mt_1$  and  $MT_2$  receptors, this putative receptor was named  $MT_3$ , according to the nomenclature recommendations of the IUPHAR (7). So far, the known inhibitors of  $MT_3$  hardly reach the nanomolar range and encompass an unusually large structural diversity of highly hydrophobic cyclic or polycyclic compounds (Refs. 5 and 6, and for review, see Ref. 3).<sup>1</sup> All pharmacological investigations on  $mt_1$ ,  $MT_2$ , and  $MT_3$  were performed using the radioligand [<sup>125</sup>I]melatonin, a ligand with high affinity for  $mt_1$  and  $MT_2$  ( $K_d = 10$ – $200$  pM) and with lower affinity for  $MT_3$  ( $K_d = 3$ – $9$  nM). The hamster kidney, liver, and brain have been used as model tissues for  $MT_3$  pharmacological studies, and our recent data confirmed that among a wide range of mammals, this rodent was indeed the best source of  $MT_3$ .<sup>1</sup> Hence, the binding specificity for [<sup>125</sup>I]melatonin competition studies on  $MT_3$  is achieved by preparing material from hamster tissues, and the fast dissociation kinetics is overcome by operating at 4 °C. In addition, iodination of the known very specific  $MT_3$  inhibitor, 5-methoxycarbonylamino-*N*-acetyltryptamine (MCA-NAT),<sup>2</sup> paved the way to more accurate and reliable investigations on  $MT_3$  (5). This ligand, combined with recently improved operating conditions, made possible for us to perform specific  $MT_3$  pharmacological studies at room temperature.<sup>1</sup> Confident in the interest of discovering novel melatoninergic pharmacological targets, we recently set up a biochemical approach to identify and characterize  $MT_3$ . The present report describes a specific purification procedure of  $MT_3$  from hamster kidney, which led to a homogeneous single protein of 26 kDa, identified by tandem mass spectrometry as a homologue of the human quinone reductase 2 (QR<sub>2</sub>, EC 1.6.99.2). This identification was confirmed by confronting  $MT_3$  pharmacological and QR<sub>2</sub> enzymatic data obtained under different cellular and biochemical conditions corresponding to  $MT_3$  or QR<sub>2</sub> typical conditions. The quinone reductase family comprises two isoforms, QR<sub>1</sub> and QR<sub>2</sub>, which have been sequenced (8, 9) and crystallized (10, 11). QR<sub>2</sub> lacks a 47-amino acid C-terminal sequence present in QR<sub>1</sub>, resulting in a differ-

Melatonin, a neurohormone produced at night in the pineal gland, is suspected to relay to the peripheral organs the circadian rhythm detected by the central nervous system. Several high affinity melatonin receptors have been identified to date, among which the  $mt_1$  (1) and  $MT_2$  (2) receptors have been cloned from human tissues. The pharmacology of these two receptors is well documented, and several compounds, including melatonin, are ligands with picomolar binding affinity (for review, see Ref. 3). Another putative melatonin receptor was

\* The costs of publication of this article were defrayed in part by the payment of page charges. This article must therefore be hereby marked "advertisement" in accordance with 18 U.S.C. Section 1734 solely to indicate this fact.

‡‡ To whom correspondence should be addressed: Pharmacologie Moléculaire et Cellulaire, Institut de Recherches Servier, 125 Chemin de Ronde, 78 290 Croissy-sur-Seine, France. Tel.: 33-1-55-72-27-48; Fax: 33-1-55-72-28-10; E-mail: jaboutin@netgrs.com.

<sup>1</sup> O. Nosjean, J. P. Nicolas, F. Klupsch, P. Delagrance, E. Canet, and J. A. Boutin, submitted for publication.

<sup>2</sup> The abbreviations used are: MCA-NAT, 5-methoxycarbonylamino-*N*-acetyltryptamine; QR<sub>2</sub>, quinone reductase 2; OG, octylglucopyranoside; BNAH, dihydrobenzyl nicotinamide; DCM, dichloromethane; HATU, *O*-(7-azabenzotriazol-1-yl)-1,1,3,3-tetramethyluronium hexafluorophosphate; S20098, agomelatine; S26553, *N*-methyl-1-[2-(acetyl amino)ethyl]naphthalen-7-yl-carbamate; S27145, *N*-[2-(7-amino-1-naphthyl)ethyl]acetamide.

TABLE I  
Purification of hamster kidney  $MT_3$

Purification of hamster kidney  $MT_3$  was monitored by  $^{125}\text{I}$ -MCA-NAT binding,  $QR_2$  enzymatic activity (menadione/BNAH in the presence of dicoumarol), and  $QR_1$  activity (menadione/NADH). Briefly, the tissue homogenate in 0.2 M sucrose (H) was centrifuged at low speed to remove nuclei and unbroken cells ( $P_1$ ), and the resulting supernatant was incubated in mild detergent conditions (5 mM OG, fraction  $S_1 + OG$ ) in order to separate cytoplasm and loosely membrane-associated material ( $S_{OG}$ ) from membranes ( $P_{OG}$ ). The cytoplasm-enriched fraction was dialyzed and fractionated by DEAE ion-exchange chromatography. The  $MT_3$ -enriched fractions were pooled and concentrated (DEAE) before final purification by affinity chromatography (affinity). Data are representative of three independent purifications performed with five hamster kidneys as starting material. The affinity eluates were used for activity assays and electrophoresis analysis. The protein content was estimated by densitometry of the electrophoregram in the presence of a bovine serum albumin quantity calibration. Binding data are expressed as fmol/mg (specific binding) or fmol (total binding) of bound ligand. Enzymatic data are expressed as nmol/min/mg (specific activity) or nmol/min (total activity).

Purification step	$MT_3$ binding assay: $^{125}\text{I}$ -MCA-NAT binding			$QR_2$ activity assay: menadione/BNAH/dicoumarol activity			$QR_1$ activity assay: menadione/NADH activity		
	Specific binding	Purification factor	Total binding	Specific activity	Purification factor	Total activity	Specific activity	Purification factor	Total activity
	fmol/mg		fmol	nmol/min/mg		nmol/min/mg	nmol/min		nmol/min
H	68	1.0	24,870	9.0	1.0	3,278	6.4	1.0	2,330
$P_1$	73	1.1	7,276	1.6	0.2	157	9.6	1.5	961
$S_1 + OG$	142	2.1	29,171	14.7	1.6	3,014	15.9	2.5	3,266
$P_{OG}$	46	0.7	3,164	2.8	0.3	194	12.7	2.0	1,583
$S_{OG}$	240	3.5	30,006	21.2	2.4	2,646	26.3	4.1	1,808
DEAE	935	13.7	18,512	112	12.5	2,220	0.8	0.1	15
Affinity	702,238	10,312	3,792	90,785	10,115	490	0	0	0

TABLE II  
 $MT_3$  pharmacological competitions and  $QR_2$  enzymatic inhibitions

$MT_3$  pharmacological competitions and  $QR_2$  enzymatic inhibitions on hamster kidney (hamster  $MT_3/QR_2$ ) and CHO- $QR_2$  (human  $QR_2$ ) nuclei-free fractions. The samples were prepared as described under "Materials and Methods," and dialyzed against 20 mM Tris-HCl, pH 7.5, 1 mM  $\text{CaCl}_2$  in order to remove the sucrose. The hamster  $MT_3/QR_2$  sample corresponded to the  $S_1$  fraction of the purification procedure. Data are expressed as  $K_i$  (nM) for binding measurements and, since the type of enzymatic competition of each compound was unknown, as  $\text{IC}_{50}$  ( $\mu\text{M}$ ) for enzymatic measurements. Menadione and BNAH enzymatic data are represented as  $K_m$  ( $\mu\text{M}$ ). All values are the means of triplicate experiments reproduced three to six times.

	$MT_3$ binding: $^{125}\text{I}$ -MCA-NAT binding, $K_i$ (nM)		$QR_2$ activity: Menadione/BNAH/dicoumarol activity, $\text{IC}_{50}$ or $K_m$ ( $\mu\text{M}$ )	
	Hamster $MT_3/QR_2$	Human $QR_2$	Hamster $MT_3/QR_2$	Human $QR_2$
Menadione	4,520 $\pm$ 853	2,338 $\pm$ 861	25.2 $\pm$ 2.6 ( $K_m$ )	8.9 $\pm$ 0.11 ( $K_m$ )
BNAH	86 $\pm$ 9.9	334 $\pm$ 124	60.8 $\pm$ 5.1 ( $K_m$ )	57.6 $\pm$ 4.1 ( $K_m$ )
Dicoumarol	2,852 $\pm$ 756	1,686 $\pm$ 590	566 $\pm$ 12	620 $\pm$ 26
Estradiol	601 $\pm$ 97	3,090 $\pm$ 253	>10,000	>10,000
2-Iodomelatonin	8.3 $\pm$ 2.3 <sup>a</sup>	11.0 $\pm$ 2.8	1.2 $\pm$ 0.3	29 $\pm$ 2.3
S26553	3.0 $\pm$ 1.0 <sup>a</sup>	62.4 $\pm$ 16.4	2.8 $\pm$ 1.8	41.4 $\pm$ 3.7
MCA-NAT	81 $\pm$ 19 <sup>a</sup>	642 $\pm$ 211	43.5 $\pm$ 7.0	376 $\pm$ 68
N-Acetylserotonin	146 $\pm$ 13.5	207 $\pm$ 19	92 $\pm$ 34	204 $\pm$ 44
Melatonin	277 $\pm$ 22 <sup>a</sup>	382 $\pm$ 99	43 $\pm$ 12	246 $\pm$ 47
Luzindole	1,156 $\pm$ 304 <sup>a</sup>	>10,000	>10,000	>10,000
Serotonin	3,563 $\pm$ 1,067	>10,000	>10,000	2,933 $\pm$ 384
Tryptamine	>10,000	>10,000	>10,000	>10,000

<sup>a</sup> These data are part of a previous report (Footnote 1).

ent substrate specificity. It is noteworthy that the literature on  $QR_2$  enzymology is rather scarce (12–14). Interestingly,  $QR_2$  was originally discovered in 1962 as a flavoenzyme (12), later re-discovered as the  $QR_1$ -related enzyme (14), and was recently found again in porcine kidney as a puromycin aminonucleoside-binding protein (15). We now unveiled a new facet of  $QR_2$  as the melatonin-binding site  $MT_3$ , opening new perspectives in melatonin investigations as well as in quinone reduction studies.

## EXPERIMENTAL PROCEDURES

### Materials

[ $^{125}\text{I}$ ]MCA-NAT (2200 Ci/mmol) was custom synthesized by Amer-sham Pharmacia Biotech (Orsay, France). 2-Iodomelatonin and MCA-NAT were purchased from Tocris (Bioblock, Illkirch, France), dihydrobenzylnicotinamide was obtained from Maybridge (Interchim, Montluçon, France), and all other reagents were obtained from Sigma-Aldrich (Saint Quentin Fallavier, France).

### Partial Purification of $MT_3$

Frozen hamster kidneys were obtained from Charles River Breeding Laboratories (Saint Aubin les Elbeuf, France). The tissues were thawed, chopped, and added to 5 ml/g of homogenization buffer (50 mM Tris-HCl, pH 7.5, 0.2 M sucrose, 1 mM  $\text{CaCl}_2$ , and Complete<sup>TM</sup> mixture of protease inhibitors). The cells were gently disrupted using a Dounce

homogenizer and unbroken material and nuclei were pelleted at 280  $\times$  g. The pellet ( $P_1$ ) was treated identically a second time and the two 280  $\times$  g supernatants were pooled ( $S_1$ ) and supplemented with 5 mM final  $\beta$ -octyl glucopyranoside (OG) prior to a 30-min incubation under agitation. Cytoplasm and loose membrane-associated material was recovered in the supernatant of a 100,000  $\times$  g centrifugation ( $S_{OG}$ ) and the pellet ( $P_{OG}$ ) was conserved for analysis. The  $S_{OG}$  fraction was dialyzed against 20 mM Tris-HCl, pH 7.5, 1 mM  $\text{CaCl}_2$  and applied to a 6  $\times$  5-cm DEAE Bio-Gel A column (Bio-Rad) pre-equilibrated with the same buffer. The elution of proteins was triggered by a stepwise gradient of 0–1 M NaCl in the application buffer and was monitored by absorbance at 280 nm. The fractions of interest were pooled and dialyzed against the application buffer, concentrated by laying the dialysis tubing onto 20,000 Da polyethylene glycol, and further dialyzed against the application buffer. All procedures were carried out at 4  $^\circ\text{C}$ . Most often, the OG solubilization sample  $S_{OG}$  was flash frozen in liquid nitrogen and stored until application on the ion-exchange phase. For binding studies, this partially purified  $MT_3$  sample was dialyzed against 20 mM Tris-HCl, pH 7.5, 1 mM  $\text{CaCl}_2$  in order to remove the sucrose which inhibited MCA-NAT binding. The final DEAE sample was frozen identically before further purification or analysis.

### Chemical Synthesis of a $MT_3$ Specific Affinity Phase

The ligand *N*-[2-(7-amino-1-naphthyl)ethyl]-acetamide (S27145, Fig. 1) was prepared in three steps from agomelatine (S20098 (16)) and attached to the polymer resin over a spacer, in two further steps, as

follows. A solution of *N*-[2-(7-methoxy-1-naphthyl)ethyl]acetamide (10 g, 41 mmol) in DCM (50 ml) was treated with  $BBr_3$  (25 ml) at  $-15^\circ C$  under nitrogen. The reaction mixture was kept at  $-15^\circ C$  for 1 h, then poured on, hydrolyzed with 1 *N*  $NaHCO_3$  and extracted with methyl-ethylketone. The organic layer was dried over sodium sulfate and concentrated. The residue was taken up with DCM (100 ml) and the precipitate collected and dried to afford 8.77 g (93%) of *N*-[2-(7-hydroxy-1-naphthyl)ethyl]acetamide (compound 1). A solution 1 (8.7 g, 38 mmol) in DCM (400 ml) was treated with triethylamine (6.9 ml, 50 mmol) and *N*-phenyl-bistrifluoromethane sulfonimide (20 g, 53 mmol). The reaction mixture was refluxed for 12 h, then cooled, concentrated, taken up with diethyl ether, washed with 1 *N*  $NaHCO_3$ , water, and then dried over magnesium sulfate. The crude product was purified on silica gel with DCM/ethyl acetate (95:5) to afford 11.5 g (84%) of *N*-[2-(7-trifluoromethylsulfoxy-1-naphthyl)ethyl]acetamide (compound 2). A mixture of 2 (4.0 g, 11 mmol) with benzophenimine (7 g, 38 mmol), bis(diphenylphosphino-1-1'-binaphthalene) (310 mg, 0.5 mmol), palladium acetate (70 mg, 0.3 mmol), and cesium carbonate (5 g, 15 mmol) in dioxane (160 ml) was refluxed under nitrogen for 12 h. The resulting reaction mixture was hydrolyzed with water and extracted with diethyl ether. The organic layer was washed with 10% citric acid and water, then dried over sodium sulfate and concentrated. The resulting crude product was dissolved in tetrahydrofuran (150 ml), treated with 1 *N* HCl (200 ml), and heated at  $60^\circ C$  for 1 h. The reaction was cooled, extracted with diethyl ether, and the aqueous phase was brought to pH 11 with NaOH, then extracted with DCM. The organic layer was dried over sodium sulfate, concentrated, and purified on silica gel in DCM/methanol (97:3) to afford 1.44 g of *N*-[2-(7-amino-1-naphthyl)ethyl]acetamide. The corresponding hydrochloride salt (1.61 g, 55%, compound 3) was obtained by treatment of the base in ethyl acetate with HCl in diethyl ether. Compound 3 (876 mg, 3.31 mmol) and 6-*tert*-butoxycarbonylamino hexanoic acid (1.15 g, 4.97 mmol) were dissolved in DCM (20 ml) and neat HATU (1.89 g, 4.97 mmol) was added in one single portion, followed by a slow addition of diisopropylethylamine (2.57 g, 14.90 mmol). After a 15-min reaction at room temperature, high performance liquid chromatography showed no remaining amine and one major new product. Ethyl acetate (100 ml) was then added and the solution washed 3 times with brine ( $3 \times 25$  ml), 1 *M* HCl ( $3 \times 25$  ml), 5%  $NaHCO_3$  ( $3 \times 25$  ml), and brine ( $3 \times 25$  ml), dried over magnesium sulfate and evaporated under vacuum. The yield of [5-[7-(2-acetylamino-ethyl)-naphthalen-2-ylcarbonyl]-pentyl]-carbamate *tert*-butyrate, compound 4 (1.4 g), was 95% and its high performance liquid chromatography purity was 99%. The Boc group was deprotected by treatment of 4 (1.40 g, 3.17 mmol) with trifluoroacetic acid (10 ml) in DCM (20 ml). After 15 min at room temperature, the solution was evaporated under vacuum and lyophilized in water/acetonitrile (9:1). The trifluoroacetic acid salt was then attached to the Novasyn TG carboxy resin (Novabiochem, 0.25 mmol/g) (12 g) on a semiautomatic synthesizer with axial shaking, using HATU (1.21 g, 3.17 mmol) in the presence of diisopropylethylamine (2.05 ml, 11.88 mmol) in a mixture of 200 ml of DCM/DMF (1:1) as solvent. The reaction mixture was shaken for 64 h at room temperature. After filtration, the usual washings were performed:  $3 \times$  with DMF and isopropyl alcohol, alternatively and 3 times with DCM. The resin was then capped by treatment with a large excess of glycine methyl ester hydrochloride (3.98 g, 31.7 mmol) using HATU (12.05 g, 31.7 mmol) in the presence of diisopropylethylamine (7.65 ml, 44.4 mmol) in 200 ml of a mixture of DCM/DMF (1:1). The same washings were performed after filtration. Estimation of the substitution level of the resin was carried out by microanalysis of the nitrogen percentage content: 0.11 mmol ligand/g of resin.

#### Complete Purification of $MT_3$

The partially purified  $MT_3$  sample was subjected to affinity chromatography at  $4^\circ C$ . The phase was synthesized as described above and used in a batch procedure. It was washed three times with 20 *mM* Tris-HCl, pH 7.5, 1 *mM*  $CaCl_2$  and mixed with the sample at a ratio of 50  $\mu g$  of protein/mg of phase. The incubation was performed for 15 min under gentle agitation after which the sedimentation of the resin was left to occur. The unbound material was removed by pipetting over the supernatant and the phase was washed twice with the equilibration buffer. The bound proteins were eluted by incubating the phase for 15 min in the equilibration buffer supplemented with 50  $\mu M$  MCA-NAT. The eluate was recovered by pipetting, dialyzed against water, and concentrated on polyethylene glycol as described above. The precipitate obtained in dry ice-cold acetone was dried under a flow of nitrogen and analyzed by Laemmli polyacrylamide gel electrophoresis (17). The proteins were detected in the gel by Coomassie Blue.

#### Mass Spectrometry Analysis of Purified $MT_3$

The protein spot in the Laemmli electrophoresis performed after affinity chromatography was excised from the Coomassie Blue-stained gel and washed with 50% acetonitrile. Gel pieces were dried in a vacuum centrifuge and reswollen in 20  $\mu l$  of 25 *mM*  $NH_4 HCO_3$  containing 0.5  $\mu g$  of trypsin (Promega, sequencing grade). After 4 h incubation at  $37^\circ C$ , the gel pieces were extracted with 5% formic acid and acetonitrile. The extracts were evaporated to dryness. The residues were dissolved in 0.1% formic acid and desalted using a Zip Tip (Millipore). Elution of the peptides was performed with 5–10  $\mu l$  of 50% acetonitrile, 0.1% formic acid solution. The peptide solution was introduced onto a glass capillary (Protana) for nano-electrospray ionization. Tandem mass spectrometry experiments were carried out on a Q-TOF hybrid mass spectrometer (Micromass, Altrincham, United Kingdom) in order to obtain sequence information. MS/MS sequence information was used for data base searching using the programs MS-Edman located at the University of California San Francisco and BLAST located at the NCBI.

#### cDNA-derived Expression of $hQR_2$ in Hamster Ovary CHO Cells and Preparation of Samples

The  $QR_2$  coding sequence was isolated by reverse transcriptase-polymerase chain reaction from human liver mRNA (CLONTECH, Palo Alto, CA) using the 5' sense primer (5'-GAATTCCTCCACCATGGCAGTAAGAAGTACTCATGTC-3', nucleotides 176–202) and the 3' antisense primer (5'-GCGGCCGCTCATTATTGCCCGAAGTGCCAGTGGCTGTGC-3', nucleotides 843–871) generated from the published sequence (Ref. 9; access number JO2888). Liver mRNA (200 ng) was reverse-transcribed with oligo(dT)<sub>12–18</sub> in accordance with the first-strand cDNA synthesis protocol from Amersham Pharmacia Biotech. Polymerase chain reactions were performed in 100  $\mu l$  containing 10 *mM* Tris-HCl, pH 8.3, 1.5 *mM*  $MgCl_2$ , 0.2 *mM* dNTP, 2  $\mu l$  of the single-stranded cDNA preparation, 0.3  $\mu M$  of each primer, and 2 units of pfu native polymerase (Stratagene) with a 35 cycles program of  $94^\circ C$  for 1 min,  $65^\circ C$  for 2 min, and  $72^\circ C$  for 2 min and a final extension at  $72^\circ C$  for 8 min. The amplified cDNA was then subcloned in-frame into *EcoRI* and *NotI* site of the pcDNA3.1(+) vector (Invitrogen, San Diego, CA). CHO-K1 cells maintained in Ham's F12 medium supplemented with 10% fetal calf serum, 2 *mM* glutamine, 500 IU/ml penicillin, and 500  $\mu g/ml$  streptomycin were transiently transfected by the pcDNA3.1(+)- $QR_2$  plasmid using LipofectAMINE as described by the manufacturer (Life Technologies). Forty-eight hours after the beginning of transfection, the adherent cells were washed by phosphate-buffered saline and harvested in 10 ml of homogenization buffer (see "Purification of  $MT_3$ ," above) and transferred from flask to flask. The cell suspension obtained was adjusted to 0.2 *M* sucrose and spun at  $280 \times g$ . The resulting nuclei-free supernatant was assayed for protein and  $MT_3/QR_2$  content.

#### Assays

All assays were performed in triplicate and data presented herein are representative of two to six individual experiments.

**Total Protein**—The protein concentration was determined by the method of Lowry (18) using bovine serum albumin as a standard.

**$MT_3$  Pharmacological Data**—The  $MT_3$  binding was performed according to our original procedure.<sup>1</sup> Briefly, 100  $\mu g$  (samples from animals) or 20  $\mu g$  (samples from CHO) of proteins were incubated at 20–22  $^\circ C$  for 10–20 min with 200 pM [<sup>125</sup>I]MCA-NAT in the presence (nonspecific binding) or absence (total binding) of 10  $\mu M$  MCA-NAT and, for competition studies, with varying concentrations of test compounds. The final volume was 150  $\mu l$  in 20 *mM* Tris-HCl, pH 7.5, 1 *mM*  $CaCl_2$ . Incubation was stopped by filtration through a 96-well filtration support disposed directly onto a Multiscreen filtering apparatus (Millipore) connected to a vacuum pump, allowing rapid filtration after the samples were loaded using a 96-well pipetting device (Transtar, Costar). The filter-associated radioactivity was measured in a  $\beta$ -scintillation counter (TopCount NXT, Packard). Samples from CHO culture and from the purification of  $MT_3$  up to the ion exchange chromatography step were analyzed on glass fiber filters (GF/B Unifilter, Packard), while elution from the ion-exchange resin was followed using polyvinylidene difluoride filters (Immobilon™ Multiscreen, Millipore) presoaked in methanol and rinsed three times by 200  $\mu l$  of binding buffer. Alternatively, samples from the final purification steps, affinity chromatography, and ion exchange chromatography as an internal reference, were assayed for  $MT_3$  binding using 96-well format size-exclusion chromatography. Eighty  $\mu l$  of dry Sephadex G-25 fine (APB) were distributed into 96-well format polyvinylidene difluoride filters (Dura-pore™ Multiscreen, Millipore) using a Multiscreen powder dispensing

apparatus. The exclusion phase was hydrated with 250  $\mu$ l of 20 mM Tris-HCl, pH 8.5, and spun at  $550 \times g$  for 1 min in a 96-well plate basket. The phase was further rinsed three times using 120  $\mu$ l of the same buffer, left to equilibrate at 4 °C for 30 min, and spun before sample application. The samples were preincubated at 4 °C during 30 min with 200 pM [ $^{125}$ I]MCA-NAT as described above, and 120  $\mu$ l of the mixture were loaded onto the exclusion phase. The plates were immediately spun at  $550 \times g$  for 1 min. The free radioligand was excluded from the eluate by diffusion in the chromatographic medium, and 90  $\mu$ l of the eluate were used for scintillation counting. For competition studies, the data presented are affinity constants ( $K_i$ ) calculated from specific binding values of logarithmic compound concentrations, according to the method of Cheng and Prusoff (19).

**QR Enzymatic Activity**—The measurements of  $QR_1$  and  $QR_2$  quinone reductase activities were adapted from Jaiswal *et al.* (9) and Zhao *et al.* (14).  $QR_1$  activity was measured using 100  $\mu$ M menadione as substrate and 100  $\mu$ M NADH as co-substrate, while  $QR_2$  activity was measured using 100  $\mu$ M menadione as substrate, 100  $\mu$ M dihydrobenzylnicotinamide (BNAH) as co-substrate, and 100  $\mu$ M dicoumarol as  $QR_1$  inhibitor. In both cases, the activities were measured at 25 °C in 200  $\mu$ l of 20 mM Tris-HCl, pH 7.5, 1 mM OG and the reactions were followed at 440 nm using the intrinsic fluorescence of the two co-substrates with excitation at 340 nm (PolarStar 96-well plate reader, BMG, Offenburg, Germany). Samples were diluted before use in the measurement buffer supplemented with 10% glycerol, in order to apply the desired amount of protein in 20  $\mu$ l. The instrument was calibrated using a range of co-substrate concentrations. The  $IC_{50}$  values were calculated from inhibition curves using semi-logarithmic plots of the compound concentrations (8 points).

## RESULTS

**Terminology and Assays of  $MT_3$  and  $QR_2$** —This work primarily focused on the melatonin-binding site  $MT_3$ , which was studied and purified using [ $^{125}$ I]MCA-NAT binding (5) as a specific assay, designated herein as the “ $MT_3$  assay.” Purification of  $MT_3$  from hamster kidney provided “partially purified  $MT_3$ ” and “ $MT_3$  purified to homogeneity.” The cloning and expression of the human  $QR_2$  gene in CHO provided an identified source of this enzyme, which was assayed using the well described oxidoreduction mechanism involving a quinone (electron acceptor) and a nicotinic derivative (electron donor). For assaying the  $QR_2$  enzymatic activity, menadione was the substrate and a commercially available fluorescent NADH analogue, dihydrobenzylnicotinamide (BNAH, Powell *et al.* (20)), was used for the first time as the co-substrate. Dicoumarol, a potent  $QR_1$  inhibitor and poor  $QR_2$  inhibitor (14) was added to the assay to ensure  $QR_2$  specificity. Control assays of  $QR_1$  activity were performed when necessary, using menadione as the substrate and NADH as the co-substrate, which provided good  $QR_1$  specificity since NADH is a very poor co-substrate for  $QR_2$  (14, 20).<sup>3</sup> Although, in the light of our results presented thereafter,  $MT_3$  and  $QR_2$  seem to designate a unique protein, for convenience in the present report, we alternatively refer to hamster  $MT_3$  or  $MT_3/QR_2$  and human  $QR_2$ , depending on the methodological approach involved.

**Purification and Identification of  $MT_3$  as  $QR_2$** —The purification of the melatonin-binding site  $MT_3$  was performed as described under “Experimental Procedures” and the intermediate fractions were assayed for [ $^{125}$ I]MCA-NAT binding and  $QR_2$  enzymatic activity.  $QR_1$  activity was also assayed in all samples as a control. We started the purification of the  $MT_3$  melatonin-binding site by preparing a nuclei-free subcellular fraction, from which  $MT_3$  was recovered with high yield in the supernatant of a 100,000  $\times g$  centrifugation after mild detergent treatment (5 mM octylglucoside). Dialysis removed most of the detergent molecules thanks to the high critical micellar concentration of OG ( $CMC_{OG} = 25$  mM (21)). The dialysate was applied to a DEAE anion exchanger, from which  $MT_3$  was eluted by a discontinuous gradient of NaCl. The  $MT_3$  contain-

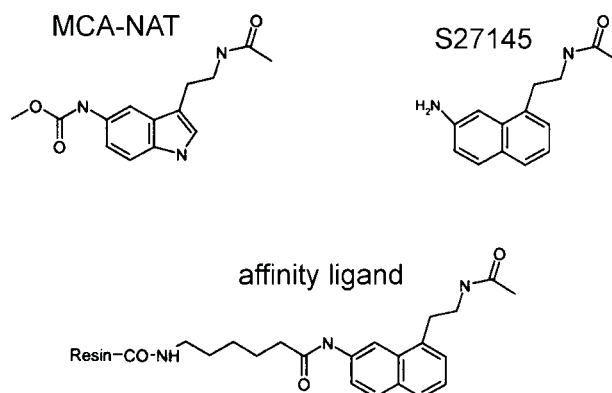


FIG. 1. Structure of MCA-NAT, S27145, and the affinity ligand [(7-[6-aminohexanoylamido]-1-naphthyl)ethyl]acetamide branched on polyethylene glycol-derived polystyrene beads through a  $C_6$  spacer.

ing fractions were pooled and dialyzed in order to remove the NaCl. Finally, we purified  $MT_3$  to homogeneity using an original affinity phase developed on the basis of the most specific  $MT_3$  ligand known to date, MCA-NAT. The synthetic ligand (S27145, Fig. 1) bears an amine function in position 7 of naphthylethylacetamide, which was substituted by a 6-aminohexanoyl moiety in order to mimic the carbonylamide function of MCA-NAT. The free amino group of the amino hexanoic spacer was used for the attachment to the affinity matrix, a polyethylene glycol-derivatized polystyrene resin. The use of a naphthyl ring eliminated the photosensitivity associated with the indole ring. The affinity chromatographic step was performed at 4 °C in a batch procedure, and the proteins specifically adsorbed on the phase were eluted by 50  $\mu$ M MCA-NAT. The eluate was analyzed by SDS-polyacrylamide gel electrophoresis, where it appeared as a single band of 26 kDa (Fig. 2). The band was recovered from the electrophoresis acrylamide gel as a trypsin digest and was analyzed by tandem mass spectrometry. The resulting five peptidic sequences were compared with protein data bases for alignment and showed 95% similarity with the human quinone reductase 2,  $QR_2$  (Fig. 3). Table I displays the yields of the successive purification steps as calculated from  $MT_3$  binding and  $QR_2$  enzymatic assay data. The [ $^{125}$ I]MCA-NAT binding data are in good agreement with the  $QR_2$  enzymatic data, with a 2.5–3.5-fold enrichment of  $MT_3/QR_2$  in the OG supernatant, and a 12.5–13.5-fold enrichment after DEAE chromatography, while  $QR_1$  was barely detectable in the ion exchange chromatography eluate. After the affinity chromatographic step, the purification of  $MT_3$ , as evaluated by [ $^{125}$ I]MCA-NAT binding and  $QR_2$  enzymatic assay, reached a 10,000-fold factor of enrichment, confirming the identity of  $MT_3$  with  $QR_2$ . Absorption and desorption of the protein preparation from the affinity medium gave a relatively low yield of recovery of  $MT_3$  and  $QR_2$  signals (about 20%), probably due to the rapid kinetics of ligand exchange of  $MT_3$ . Indeed, the dissociation constant at room temperature is about  $0.3$  s<sup>-1</sup>,<sup>1</sup> and performing the affinity chromatographic step at 4 °C could not completely counterbalance the rapid dissociation kinetics.

**Cloning, Overexpression, and Tissue Distribution of  $QR_2$** —The human  $QR_2$  gene was amplified from total RNA of human liver (9) and was used for the preparation of CHO cells transiently expressing  $QR_2$ . Four clones were prepared and transfected in CHO cells.  $MT_3$  binding as well as  $QR_2$  enzymatic activity were assayed on a nuclei-free fraction obtained as described under “Experimental Procedures.” Data in Fig. 4 show an average of 33-fold increase in [ $^{125}$ I]MCA-NAT binding in CHO- $QR_2$ , and an average of 259-fold increase in  $QR_2$  activity as compared with native CHO cells. Hence, the amplifica-

<sup>3</sup> O. Nosjean and J. A. Boutin, unpublished observations.

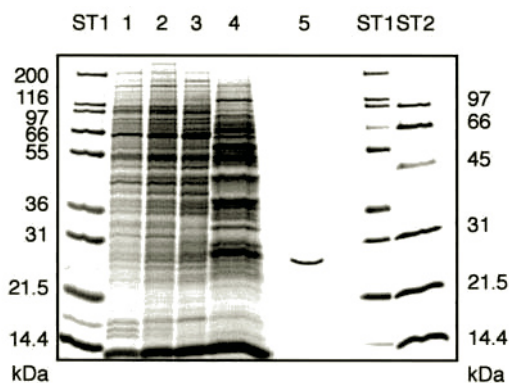


FIG. 2. Purification of  $MT_3$  from Syrian golden hamster kidney followed by SDS electrophoresis. 20  $\mu$ g of proteins was applied to each lane, except for lane 5 where the amount applied was evaluated at 400 ng by densitometry. Lane 1, Dounce homogenate; lane 2, nuclei-free fraction ( $S_1$ ); lane 3, cytosol-enriched fraction ( $S_{OG}$ ); lane 4, 30–40 mM NaCl DEAE eluate containing  $MT_3$ ; lane 5, affinity chromatography eluate, ST1 Novex molecular weight standards, ST2 Bio-Rad molecular weight standards. The affinity chromatography eluate was dialyzed against deionized water, concentrated in its dialysis tubing on high molecular weight polyethylene glycol, precipitated by dry ice-cold acetone, dried under a flow of nitrogen, and redissolved in 10  $\mu$ l of deionized water. Values in the margins indicate molecular weights in kDa; left scale, Novex molecular weight markers, right scale, Bio-Rad molecular weight markers. The gel was stained by Coomassie Blue.

```

MAGKKVLIVYAHQEPKSFNGSLKNVAVDLSRQGCTVTVSDLYAMNFE
  VLLLYAHQEPFSFNGSLK
PRATDKDITGTLNPEVFNYGVETHEAYKQRSLSADITDEQKKVREAD
  YGLEAYEAYK   TSDLLEEQR
LVIFQFPLYWFSVPAILKGMWDRVLCQGFAPDIPGFYDSGLLQCKLAL
  LAL
LSVTTGGTAEMYTKTGNGDSRYFLWPLQHGTLHFCKFKVLAPQISFA
  LSLITGGTAEMYTK   VLAPQLSFG
PEIASEEERKGMVAAWSQRLQTIWKEEPICTAHWHFQG
  LDVSSEEEER

```

FIG. 3. Sequence alignment between human  $QR_2$  and the peptide fragments obtained after purification of  $MT_3$ . First line, sequence of quinone reductase 2 from *Homo sapiens* (Swiss Prot P16083). Second line, sequence information obtained by tandem mass spectrometry on affinity purified  $MT_3$ . For these sequences, L represents either leucine (L) or isoleucine (I) since these two amino acids have the same nominal mass. For the same reason, Q represents either glutamine (Q) or lysine (K). Light shade, amino acid homolog to its counterpart in the  $QR_2$  sequence. Heavy shade, amino acid identical to its counterpart in the  $QR_2$  sequence.

tion of  $QR_2$  in CHO cells led to a strong increase of both  $MT_3$  and  $QR_2$  specific signals. The lower amplification rate observed with [ $^{125}$ I]MCA-NAT binding was probably due to an overestimation of  $MT_3$  in native CHO cells (5 fmol/mg), because this value fell within the high background level obtained with the binding technique developed for  $MT_3$  (20–30% specific signal of total).

**Ligand Specificity for  $MT_3$  and  $QR_2$  Assays**—Several series of compounds were tested for their potency to inhibit either [ $^{125}$ I]MCA-NAT binding ( $MT_3$  assay) or menadione/BNAH oxidoreduction ( $QR_2$  assay) on hamster kidney-purified  $MT_3$ / $QR_2$  and on transfected human  $QR_2$  (Table II). The  $MT_3$  ligands showed an affinity for hamster  $MT_3$ / $QR_2$  in the nanomolar range. Iodomelatonin was the most potent ligand, but also bound very tightly to  $mt_1$  and  $MT_2$ . As expected, melatonin and other melatoninergic compounds displayed no or low affinity for  $MT_3$ / $QR_2$ . The  $QR_2$  co-substrate BNAH was a ligand as

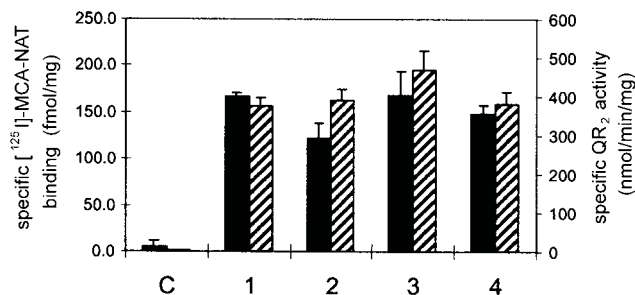


FIG. 4. [ $^{125}$ I]-MCA-NAT binding (plain bars) and  $QR_2$  enzymatic activity (striped bars) of control (C) and  $QR_2$  transfected (1–4) CHO cells. The four clones were prepared as described under “Experimental Procedures,” transfected in CHO-K1 cells and the cells were cultured for 2 days before harvesting. The cells were gently disrupted and the nuclei fraction was removed by a 280  $\times$  g centrifugation. Specific assays were performed in triplicates on the resulting fraction.

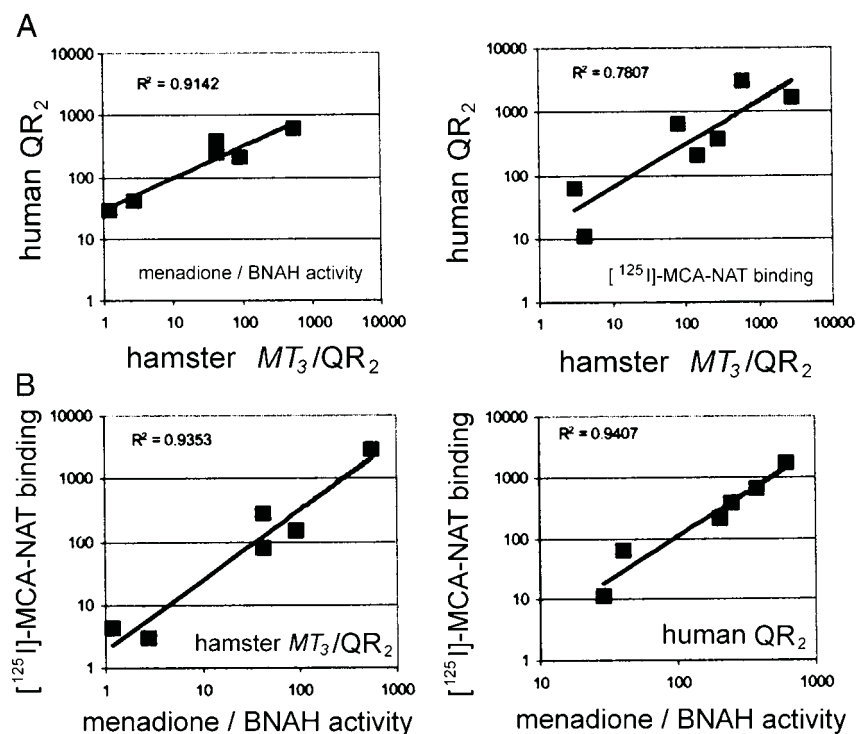
potent as MCA-NAT, while, surprisingly, menadione displayed only poor affinity for hamster  $MT_3$ / $QR_2$ . Dicoumarol, known to poorly inhibit  $QR_2$  (14) exhibited poor affinity for  $MT_3$ / $QR_2$ , while estradiol, which diminishes quinone reductase activity in Syrian hamster kidney (22), had an intermediate affinity (about 600 nM).

The pattern of inhibition of [ $^{125}$ I]MCA-NAT binding described above for hamster  $MT_3$ / $QR_2$  was conserved when the same assay was applied to a human  $QR_2$  preparation. Nonetheless, the compounds exhibited a 2–20-fold lower affinity for human  $QR_2$  compared with hamster  $MT_3$ / $QR_2$ . This hamster/human difference was also observed with the enzymatic data, where  $IC_{50}$  were 1.5–20-fold higher with human  $QR_2$  compared with hamster  $MT_3$ / $QR_2$ . Besides, hamster  $MT_3$ / $QR_2$  and human  $QR_2$  had a similar Michaelis affinity for menadione and BNAH, with a  $K_m$  of about 60  $\mu$ M for BNAH, comparable with the  $K_m$  of NAD(P)H for  $QR_1$  (20, 23). Dicoumarol was confirmed as a poor inhibitor of  $QR_2$ , with an  $IC_{50}$  of about 600  $\mu$ M. Interestingly, the  $MT_3$  compounds proved to be relatively good inhibitors of the enzyme, especially of the hamster preparation where the  $IC_{50}$  of iodomelatonin and S26553 were in the micromolar range, well below the  $K_m$  of the substrates. On the contrary, and similarly to the binding data, the  $mt_1$ / $MT_2$  ligands did not inhibit the  $QR_2$  enzymatic activity.

## DISCUSSION

The first in-depth biochemical investigation of  $MT_3$ , which was previously known solely on the basis of its peculiar melatoninergic pharmacological profile, and was often compared with the two well described  $mt_1$  and  $MT_2$  melatonin membrane receptors (4–7, 24) is reported here. The  $MT_3$  melatonin-binding site was purified to homogeneity using classical biochemical tools, and was identified by partial peptide sequencing as the homologue of the human quinone reductase 2, with 57 out of 71 amino acid identity. Furthermore, several clues support the identification of  $MT_3$  as the hamster homologue of  $QR_2$ . First,  $MT_3$  has always exhibited enzyme-like kinetics of association/dissociation of its ligands (5, 6), which has long been a hint to its pharmacological characterization with classical techniques. The identification of  $MT_3$  as an enzyme therefore explains this point. Second, both  $MT_3$  and  $QR_2$  showed hydrophobic properties, while not behaving as genuine membrane proteins. Indeed, when hamster kidney membranes were prepared in the absence of detergent,  $MT_3$  loosely associated with membrane components and fractionated almost equally in the pellet and in the supernatant of an ultracentrifugation.<sup>3</sup> This is consistent with the elution from the DEAE column at low ionic strength (30–40 mM NaCl), and with the previously described hydrophobic properties of  $QR_2$  (9, 14, 20, 25). Third, the present

FIG. 5. Comparative data obtained from pharmacological competition and enzymatic inhibition measurements performed on DEAE-purified hamster  $MT_3/QR_2$  and overexpressed human  $QR_2$ . Data are represented as follows. A, left panel, correlation of enzymatic data from hamster  $MT_3/QR_2$  (horizontal) versus human  $QR_2$  (vertical), right panel, correlation of pharmacological data from hamster  $MT_3/QR_2$  (horizontal) versus human  $QR_2$  (vertical). B, left panel, correlation of enzymatic (horizontal) versus pharmacological (vertical) data from hamster  $MT_3/QR_2$ , and right panel, correlation of enzymatic (horizontal) versus pharmacological (vertical) data from human  $QR_2$ . Data are extracted from Table II, except for substrates (menadione and BNAH) and very low affinity compounds ( $K_i$  or  $IC_{50} > 10,000$ ).



purification shows a good correlation between the purification factors calculated from “ $MT_3$  data,” *i.e.* [ $^{125}$ I]MCA-NAT binding, and from “ $QR_2$  data,” *i.e.* menadione enzymatic reduction. This observation is of particular interest regarding the last step of purification which led to a 10,000-fold enrichment of both [ $^{125}$ I]MCA-NAT binding and  $QR_2$  activity. Fourth, the affinity step which purified  $QR_2$  to homogeneity was designed on the basis of a typical  $MT_3$  ligand, MCA-NAT, which had poor structural similarity with either  $QR_2$  substrates or inhibitors known to date. Nevertheless, these observations clearly called for additional data showing the correlation between the presence of  $MT_3$  and  $QR_2$  signals. For this purpose, the human  $QR_2$  gene was inserted in a vector and transfected in CHO cells, leading to the apparition of both  $MT_3$  and  $QR_2$  phenotypes, which were otherwise absent in native cells. In itself, this result definitively associated  $MT_3$  and  $QR_2$  signals, and led to the unambiguous identification of  $MT_3$  as the hamster homologue of the human  $QR_2$ .

Thereafter, it was of particular interest to compare the properties of  $MT_3$  ligands (iodomelatonin, MCA-NAT, S26553, *N*-acetylserotonin, and melatonin),  $mt_1$ - and  $MT_2$ -specific melatoninergic ligands (luzindole, serotonin, and tryptamine), and  $QR$ -active compounds (menadione, BNAH, dicoumarol, and estradiol) toward hamster  $MT_3/QR_2$  and human  $QR_2$  in order to build up relevant cross-comparisons. The [ $^{125}$ I]MCA-NAT binding and the  $QR_2$  enzymatic data were in good agreement altogether, and the compounds evaluated showed similar relative affinities for hamster  $MT_3/QR_2$  and human  $QR_2$ . Nevertheless, it is noteworthy that there was a 2–20-fold higher affinity of the compounds for hamster  $MT_3/QR_2$  relative to human  $QR_2$ , most probably due to interspecies difference in the protein sequence and properties, as was already reported for a rat to human  $QR_1$  comparison (26). Besides, the two  $QR_2$  substrates, menadione and BNAH, displayed very contrasted affinities to hamster  $MT_3/QR_2$  and human  $QR_2$ , the former being a poor competitive inhibitor of [ $^{125}$ I]MCA-NAT binding. These differences in binding affinities may reflect the difference of behavior of these two compounds toward the catalytic site of  $MT_3/QR_2$ . Indeed, we suggest that menadione has a low affinity for a reduced FAD-

containing enzyme which seems to be present in binding experiments, while in contrast BNAH has a higher affinity for the protein bearing this intermediate catalytic site.

Furthermore, all the values for the inhibition of [ $^{125}$ I]MCA-NAT binding were in the nanomolar range, while those of menadione/BNAH oxidoreduction were in the micromolar range. As these parameters are not often compared, this difference of 3 orders of magnitude is surprising at first glance. However, when making such a comparison, one must bear in mind the dynamic ping-pong mechanism occurring at the active site, as opposed to the simple ligand exchange occurring in the binding experiments. For this reason, comparison of absolute affinity constants is not relevant, in contrast to correlation representations. Indeed, Fig. 5 shows a good correlation between the data discussed above, whether the comparison applies to the enzymatic (Fig. 5A, left panel) or binding (Fig. 5A, right panel) data from hamster  $MT_3/QR_2$  and human  $QR_2$ , or conversely, when it applied to the binding and enzymatic data obtained on hamster  $MT_3/QR_2$  (Fig. 5B, left panel) or human  $QR_2$  (Fig. 5B, right panel) preparations.

In conclusion, we have purified to homogeneity the hamster kidney melatonin-binding site  $MT_3$ , which, after sequencing by mass spectrometry, was identified as the hamster homologue of the human quinone reductase 2 (EC 1.6.99.2). It was further demonstrated an overall good correlation between data collected from [ $^{125}$ I]MCA-NAT binding ( $MT_3$  specific assay) and from menadione/BNAH + dicoumarol oxidoreduction ( $QR_2$  specific assay) experiments. The purification scheme led to a 10,000-fold enrichment in both the  $MT_3$  binding and the  $QR_2$  activity, and we showed that  $QR_2$  activity and  $MT_3$  binding both appeared after  $QR_2$  transfection in CHO cells. Furthermore, we found that inhibition data obtained with various compounds classically involved in  $MT_3$  or  $QR_2$  inhibition were correlated. Taken together, these results show that the former putative melatonin-binding site  $MT_3$  is now identified as the quinone reductase  $QR_2$ . The relative abundance of the  $MT_3$  signal ([ $^{125}$ I]melatonin and, more specifically, [ $^{125}$ I]MCA-NAT binding) in hamster organs compared with other mammals has tempered the pharmacological interest of this melatonin-bind-

ing site to date. It is now suggested that hamster  $QR_2$  has an inhibition specificity different enough from human  $QR_2$  to have appeared until now as a distinct protein called  $MT_3$ , being in fact only an inter-species homologue. Furthermore, hamster  $MT_3/QR_2$  and, to a lower extent, human  $QR_2$ , show interesting binding affinities for melatonin and  $MT_3$ -specific ligands. The oxidoreductive properties of the  $QR_2$  open the way for a novel enzymatic investigation of the highly debated antioxidant properties of melatonin (for review, see Ref 27). Hence, in addition to the G protein-coupled receptors of melatonin ( $mt_1$  and  $MT_2$ ) and the transferase arylalkylamine *N*-acetyltransferase which controls the limiting step of melatonin biosynthesis (28),  $MT_3/QR_2$  appears as a fourth molecular target to explore the multiple facets of melatonin action.

*Acknowledgment*—We are indebted to Hervé Rique for the artwork.

#### REFERENCES

1. Reppert, S. M., Weaver, D. R., and Ebisawa, T. (1994) *Neuron* **13**, 1177–1185
2. Reppert, S. M., Godson, C., Mahle, C. D., Weaver, D. R., Slaugenhaupt, S. A., and Gusella, J. F. (1995) *Proc. Natl. Acad. Sci. U. S. A.* **92**, 8734–8738
3. Dubocovich, M. L. (1995) *Trends Pharmacol. Sci.* **16**, 50–56
4. Duncan, M. J., Takahashi, J. S., and Dubocovich, M. L. (1988) *Endocrinology* **122**, 1825–1833
5. Molinari, E. J., North, P. C., and Dubocovich, M. L. (1996) *Eur. J. Pharmacol.* **301**, 159–168
6. Paul, P., Lahaye, C., Delagrangre, P., Nicolas, J. P., Canet, E., and Boutin, J. A. (1999) *J. Pharmacol. Exp. Ther.* **290**, 334–340
7. Dubocovich, M. L., Cardinali, D. P., Guardiola-Lemaître, B., Hagan, R. M., Krause, D. N., Sugden, B., Vanhoutte, P. M., and Yocca, F. D. (1998) in *The IUPHAR Compendium of Receptor Characterization and Classification*, pp. 187–193, IUPHAR Media, London
8. Jaiswal, A. K., McBride, O. W., Adesnik, M., and Nebert, D. W. (1988) *J. Biol. Chem.* **263**, 13572–13578
9. Jaiswal, A. K., Burnett, P., Adesnik, M., and McBride, O. W. (1990) *Biochemistry* **29**, 1899–1906
10. Li, R., Bianchet, M. A., Talalay, P., and Amzel, L. M. (1995) *Proc. Natl. Acad. Sci. U. S. A.* **92**, 8846–8850
11. Foster, C. E., Bianchet, M. A., Talalay, P., Zhao, Q., and Amzel, L. M. (1999) *Biochemistry* **38**, 9881–9886
12. Liao, S., Dulaney, J. T., and Williams-Ashman, H. G. (1962) *J. Biol. Chem.* **237**, 2981–2987
13. Jaiswal, A. K. (1994) *J. Biol. Chem.* **269**, 14502–14508
14. Zhao, Q., Yang, X. L., Holtzclaw, W. D., and Talalay, P. (1997) *Proc. Natl. Acad. Sci. U. S. A.* **94**, 1669–1674
15. Kodama, T., Wakui, H., Komatsuda, A., Imai, H., Miura, A. B., and Tashima, Y. (1997) *Nephrol. Dial. Transplant.* **12**, 1453–1460
16. Depreux, P., Lesieur, D., Mansour, H. A., Morgan, P., Howell, H. E., Renard, P., Caignard, D. H., Pfeiffer, B., Delagrangre, P., and Guardiola, B. (1994) *J. Med. Chem.* **37**, 3231–3239
17. Laemmli, U. K. (1970) *Nature* **227**, 680–685
18. Lowry, O. H., Roseborough, N. J., Farr, A. L., and Randall, R. J. (1951) *J. Biol. Chem.* **193**, 265–275
19. Cheng, Y. C., and Prusoff, W. H. (1973) *Biochem. Pharmacol.* **22**, 3099–3108
20. Powell, M. F., Wong, W. H., and Bruise, T. C. (1982) *Proc. Natl. Acad. Sci. U. S. A.* **79**, 4604–4608
21. Helenius, A., McCaslin, D. R., Fries, E., and Tanford, C. (1979) *Method. Enzymol.* **56**, 734–749
22. Roy, D., and Liehr, J. G. (1988) *J. Biol. Chem.* **263**, 3646–3651
23. Friedlos, F., Jarman, M., Davies, L. C., Boland, M. P., and Knox, R. J. (1992) *Biochem. Pharmacol.* **44**, 25–31
24. Pickering, D. S., and Niles, L. P. (1990) *Eur. J. Pharmacol.* **175**, 71–77
25. Prochaska, H. J., and Talalay, P. (1986) *J. Biol. Chem.* **261**, 1372–1378
26. Chen, S., Clarke, P. E., Martino, P. A., Deng, P. S., Yeh, C. H., Lee, T. D., Prochaska, H. J., and Talalay, P. (1994) *Protein Sci.* **3**, 1296–1304
27. Poeggeler, B. (1999) in *Reactive Oxygen Species in Biological Systems* (Gilbert, D. L., and Corton, C. A., eds) pp. 421–451, Kluwer Academic/Plenum Publishers, New York
28. Ferry, G., Loynel, A., Kucharczyk, N., Bertin, S., Rodriguez, M., Delagrangre, P., Galizzi, J.-P., Jacoby, E., Volland, J.-P., Lesieur, D., Renard, P., Canet, E., Fauchère, J.-L., and Boutin, J. A. (2000) *J. Biol. Chem.* **275**, 8794–8805